Lawrence Berkeley Laboratory
UNIVERSITY OF CALIFORNIA

Materials & Chemical Sciences Division

Presented at the U.S.–Japan Seminar:
Electronic Structure and Lattice Defects
in Alloys, Honolulu, HI, May 4–7, 1987,
and to be published in the Proceedings

Electronic Structure and Phase Stability of Alloys

D. de Fontaine

October 1987

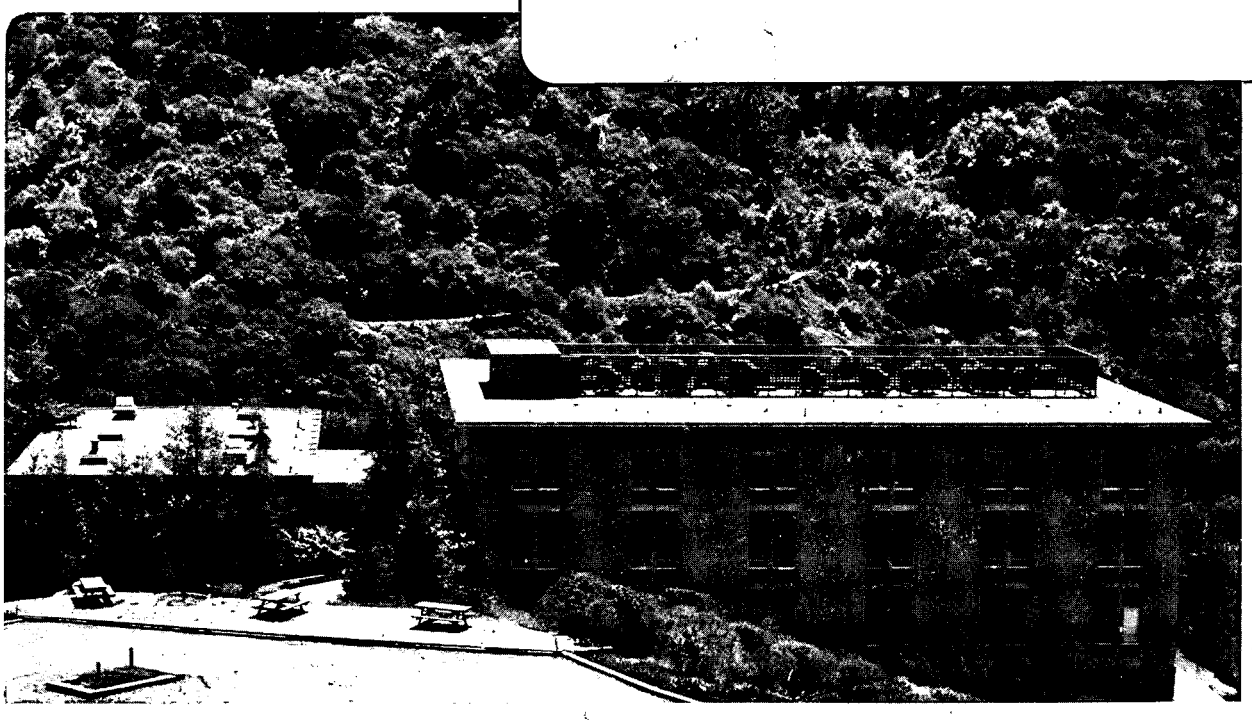

Prepared for the U.S. Department of Energy under Contract DE-AC03-76SF00098

DISCLAIMER

ELECTRONIC STRUCTURE AND PHASE STABILITY OF ALLOYS

D. de Fontaine
Department of Materials Science
and Mineral Engineering
University of California
and Lawrence Berkeley Laboratory
Berkeley, CA 94720

ABSTRACT

The computation of phase diagrams from first principles requires the combination of very precise quantum mechanical, statistical mechanical, and ground state calculations. Various methods of accomplishing this task are reviewed, such as the Gautier and Ducastelle Generalized Perturbation Method and the cluster inversion method of Connolly and Williams. As an example of the former, a calculation of the Ti-Rh phase diagram is presented.

1. INTRODUCTION

The exciting possibility now exists of deriving certain classes of alloy phase diagrams from first principles. The task is a very challenging one, but well worth the effort: no serious work on alloy systems can be carried out without knowledge of the phase diagram. In practice, phase diagrams are determined empirically, but knowledge is often fragmentary, and even in cases where it is complete and reliable, theoretical understanding of the whys and wherefores of phase equilibria is lacking.

In recent years, quantum mechanical calculations of electronic states in solids and statistical thermodynamical methods have progressed in parallel mode. The tasks of merging the quantum and statistical mechanics in a coherent whole is only just being undertaken, but already shows great promise. In this paper, we shall show along which lines the global theory is being developed, and an example of a recent binary phase diagram calculation will be given. The several aspects of the theory will be taken up in the following sections: structural aspect (Sect. 2), statistical aspect (Sect. 3), energy aspect (Sect. 4), application to phase diagram calculations (Sect. 5).

2. STRUCTURAL ASPECT

Most pure metals crystallize in the cubic structures fcc or bcc, or in the hexagonal close packed structure. Metallic alloys exhibit, in addition, a bewildering variety of crystal structures. Intermetallic compounds can be grouped in two broad classes (I) ordered superstructures of the parent structures (lattices) fcc, bcc, hcp, and (II) "interloper" structures which are not manifestly related to the parent lattices.

Thanks to the pioneering work of Kanamori [1] Cahn [2] and collaborators, understanding of ordered superstructures (class I) has progressed considerably over the past few years. Basically, the problem consists in determining those ordered arrangements of A and B atoms on lattice sites which minimize the ordering energy E_{ord} expressed as a sum of *effective pair interactions* (EPI) or multisite interactions. In principle, the problem can be solved exactly. In practice, major difficulties are encountered, such as the appearance of "nonconstructible" or infinitely degenerate structures [3]. Nevertheless, all fcc and bcc superstructures stable for the set $\{V_1,V_2\}$ of nearest neighbor (nn) and next nearest neighbor (nnn) interactions has been determined exactly [1,2]. Also, a large number of stable fcc superstructures has been derived for the set of $\{V_1,V_2,V_3,V_4\}$ of EPI up to fourth neighbors [4]. A similar study has recently been completed for bcc superstructures [5], and for a restricted set of hcp superstructures [6]. Superstructures stable for multiatom interactions have also been considered [7].

For a given parent lattice, superstructures can be classified further into *special point families* related to the wave vector of the most unstable concentration wave [8-10]. To which family a given alloy belongs, in a certain range of concentrations, depends on the ratio of the values of the EPI's in that range.

By constrast, little can be done about predicting "interloper" structures (class II): there is no fixed lattice framework to refer to, in fact, there exists a non-denumerable infinity of possible crystal structures for even binary alloys. Certain empirical schemes have been proposed for *a posterioni* rationalizing the stability of the most familiar structures [11]. In a rigorous treatment, however, the only alternative is to perform as many *ab initio* total energy calculations as deemed feasible, and to compare energies. That can be a formidable undertaking.

3. STATISTICAL ASPECT

In the previous section, perfectly ordered states only were considered. In alloys, particularly at high temperatures, elemental crystals and compounds often tolerate some departure from stoichiometric composition, and/or order can be incomplete. In fact, for the purpose of calculating phase diagrams, it is imperative to describe accurately such states of partial order.

It is obviously impractical to specify the occupation σ_p (+1 if atom A is at site p, -1 if B is at p) of every single site in the alloy. Hence, suitable averages must be carried out. Thus, a density function $\rho(\sigma)$ must be defined, which gives the probability of finding a specified configuration $\{\sigma\}$ in a very large ensemble of systems (a binary alloy, AB in our example). At equilibrium, the density function is given by the well known statistical mechanical formula

$$\rho(\sigma) = Z^{-1} e^{-E(\sigma)/k_B T} \qquad (1)$$

with partition function

$$Z = Tr^{(N)}\ e^{-E(\sigma)/k_B T} \qquad (2)$$

where $E(\sigma)$ is the energy of a particular configuration (σ), and k_BT has its usual meaning. In Eq. (2), $Tr^{(N)}$ is merely a short hand notation for the sum over all configurations of the system consisting of N atomic sites. Equations (1) and (2) are exact, but the large summation in Eq. (2) cannot be carried out for most systems of practical interest.

Several approximate techniques exist for finding explicit analytical expressions for the partitions function or, rather, for the free energy. High and low temperature expansions can be used, and Monte Carlo techniques [12] are often carried out, especially now that vast digital computing power is available. An analytical method which has been increasingly used recently is the Cluster Variation Technique (CVM) first proposed by Kikuchi [13] in 1951 and first employed for phase diagram calculations by Van Baal in 1973 [14]. The CVM provides a hierarchy of "cluster" approximations to the ordering energy and to the configurational entropy. The lowest approximation, that pertaining to clusters reduced to single points, is the Gorsky-Bragg-Williams approximation, still being utilized today in empirical treatments.

In a recent formulation of the CVM [15], the state of order of, say, a binary crystalline solid solution is described by a complete set of orthonormal functions (CONS) which are products of σ over the clusters sites. Thus, the function pertaining to cluster α is

$$\Phi_\alpha(\sigma_\alpha) = \sigma_1\sigma_2\ldots\sigma_n \qquad (3)$$

n_α being the number of points in the cluster. Any function of configuration can be expressed as an expansion in such orthogonal functions. In particular, the density function can be written

$$\rho(\sigma) = \rho_N^{\bullet}[1 + \sum_\alpha \Phi_\alpha(\sigma)\xi_\alpha] \qquad (4)$$

where $\rho_N^{\bullet}$ is the normalization 2^{-N} and the ξ_α are ensemble averages of cluster functions:

$$\xi_\alpha = \langle\Phi_\alpha(\sigma)\rangle \quad . \qquad (5)$$

These ξ form a set of linearly independent configuration variables which can be interpreted as *correlation functions*: point, pair, triplet, quadruplet... By Eq. (4), the description of the state of order now reduces to specifying the ξ's up to some largest cluster α_m. Formula (4) can be applied to partial densities, or cluster concentrations [16]

$$\rho_\beta(\sigma_\beta) = \rho_\beta^{\bullet}[1 + \sum_{\alpha\subset\beta}\Phi_\alpha(\sigma_\beta)\xi_\alpha] \qquad (6)$$

where the sum is extended to all subclusters α of the β cluster considered, with $\rho_\beta^{\bullet}=2^{-n_\beta}$. Cluster concentrations, which appear explicitly in the CVM configurational entropy are thus expressed linearly as a function of the correlations ξ, the number of such independent variables being equal to the total number of subclusters contained in the maximum cluster(s) retained in the orthonormal set expansion.

4. ENERGY ASPECT

The internal energy E can be written as a functional of the density ρ as follows

$$E[\rho] = \mathrm{Tr}^{(N)}\ \rho(\sigma)E(\sigma). \tag{7}$$

When the density function has the equilibrium distribution given by Eq. (1), then $E[\rho]$ is the correct expectation value of the energy. Inserting expression (4) for the density ρ into (7) then yields

$$E = \varepsilon_o + \sum_\alpha \varepsilon_\alpha \xi_\alpha \tag{8}$$

with configuration-independent term

$$\varepsilon_o = \rho_N^\circ\ \mathrm{Tr}^{(N)}\ E(\sigma) \tag{9}$$

and effective cluster interaction parameters

$$\varepsilon_\alpha = \rho_N^\circ\ \mathrm{Tr}^{(N)}\ \Phi_\alpha(\sigma)E(\sigma). \tag{10}$$

The meaning of Eq. (10) is best understood by considering pair interactions, say the pair consisting of a site at p and one at q. By breaking up the $\mathrm{Tr}^{(N)}$ in (10) into two parts, one over the points p and q, one over all other points, one obtains [7]

$$V_n \equiv \varepsilon_{pq} = \frac{1}{4}(V_{AA} + V_{BB} - 2V_{AB}) \tag{11}$$

where, for pairs, V_n is customarily written in place of ε_{pq} if the (pq) represents the nth neighbor pair. In Eq. (11), "pair energies" are given by

$$V_{IJ} = \rho_{N-2}^\circ\ \mathrm{Tr}^{(N-2)}\ E(I,J;\sigma') \tag{12}$$

where $E(I,J;\sigma')$ designates the energy of a configuration consisting of atom I (A or B) at p and J at q, and σ' elsewhere, the sum being carried out over all of these σ' configurations. Thus, V_{IJ} represents the energy of pair (IJ) embedded in a completely disordered average medium. It is very important to note that the energy $E(\sigma)$ of the alloy in a given configuration is *not* evaluated as a sum of pair (or even multiplet) interactions; it is merely the ordering energy E_{ord} which is expressed by means of effective pair interactions through Eq. (11).

Since *all* configurations are summed over in Eqs. (9) and (10), ε_o and ε_α, hence V_{IJ} or V_n are strictly concentration-independent. There is another way of performing averages, however: for large N, the density ρ in Eq. (7) will be sharply peaked about the average concentration c ($=c_B$, $c_A=1-c$) so that the Tr may be replaced by a sum over those configurations which have specified concentration c^*. Formally, equations similar to Eq. (8) to (12) follow in like

manner, but now $\varepsilon_o^\bullet$ and $\varepsilon_\alpha^\bullet$, also the $V_n^\bullet$ are concentration dependent, as indicated by the superscript.

It is possible to rewrite Eq. (8) in a more useful form by first noting that the energy of the completely disorderd state of concentration $c^\bullet$ is given by

$$E_{dis}^n = \varepsilon_o^\bullet + \sum_\alpha \varepsilon_\alpha^\bullet \, (\xi_p)^{n\alpha} \tag{13}$$

since, in the disordered state, all (small) cluster correlations are products of point (p) correlations $\xi_p = c_A^\bullet - c_B^\bullet$, provided that all lattice points are equivalent in the disordered phase. By eliminating $\varepsilon_o^\bullet$ from Eq. (13) and Eq. (8) written in concentration-dependent form, one gets

$$E = E_{dis} + E_{ord} \tag{14}$$

with

$$E_{ord} = \sum_\alpha \varepsilon_\alpha^\bullet \, \delta\xi_\alpha \tag{15}$$

where $\delta\xi_\alpha$ is the difference between cluster correlations in the ordered and completely disordered states. This approach is the one taken by Sigli and Sanchez [18], following the prescription suggested by the generalized perturbation method (GPM) of Gautier and Ducastelle [19].

In practice, the state of order will be defined by just a few cluster functions of the complete orthonormal set. Correspondingly, the internal energy expansions (8) or (15) will be limited to a few small-cluster interactions. The problem of convergence of the energy expressions has not been resolved, although it has been argued that convergence should be more rapid with concentration-dependent interactions [$\varepsilon_\alpha^\bullet$, Eq. (15)] than with concentration independent ones [ε_α, Eq. (8)].

A difficult problem remains: that of determining the values of the EPI's (or cluster interactions). Electronic band structure methods currently exist for performing accurate first-principles calculations of pure elemental crystals or stoichiometric compounds using, as input, only presumed crystal structures and the atomic numbers Z_A, Z_B. It is also possible to derive self consistently a perfectly disordered crystalline solid solution of given average concentration by a method known as the coherent potential approximation (CPA) [20]. The CPA has been implemented in tight binding (TB-CPA) [21] or Korringa-Kohn-Rostoker (KKR-CPA) [22] schemes.

Accordingly, two general methods exist for calculating cluster interactions: one takes as its starting point the fully ordered states, the other takes the fully disordered state as its starting point. The former, based on Eq. (8), yields concentration independent ε_α parameters (in the absence of elastic energy corrections), the latter, based on Eq. (15), yields concentration dependent $\varepsilon_\alpha^\bullet$ parameters.

According to the first of these scenarios, originally proposed by Connolly and Williams [23], one calculates, as accurately as possible, the total energies

of as many structures, or rather superstructures, as there are parameters ε_α to be determined. Consider the fcc case in the nn tetrahedron approximation of the CVM. The sum in Eq. (8) is then limited to the tetrahedron and its subclusters: the nn triangle, nn pair and point. The structure-independent term ε_0 must also be determined, hence 5 structures must be examined. Usually, one takes pure A, pure B (both fcc), A_3B ($L1_2$ structure), AB ($L1_0$) and AB_3 ($L1_2$). Recently [24], this method has been applied to the case of noble metal alloys (Cu, Ag, Au): total energies were calculated for the 5 structures by ASW methods and elastic energy was incorporated by taking into account the change of lattice parameters with alloy composition. Thus, a concentration dependence was indirectly introduced in the interaction energies. In this way, Terakura and co-workers [24] were able to explain, in at least a semi-quantitive way, the remarkable thermodynamic differences observed in the three binaries Cu-Ag, Cu-Au and Ag-Au. The Connolly and Williams method has also been applied to semiconductor compounds by Zunger et al. [23].

As mentioned, the second method takes the fully disordered state as its starting point. The cluster interactions are obtained by perturbing the CPA medium, either in k-space [19] or real space formulations [26]. The coefficients of the resulting expansions, which make use of the off-diagonal elements of the CPA Green's function, are related directly to the ε^*_α interactions which are then inherently concentration dependent. Gautier and Ducastelle [19] have called their method the generalized perturbation method (GPM), and it has been used successfully in the tight binding approximation framework for transition metal alloy systems [26]. Remarkable agreement has been found by Sigli and Sanchez [27] between calculated and experimental values of the heat of mixing of bcc transition metal alloy systems. The GPM has also been implemented on the KKR-CPA [28], resulting, for example, in cluster interactions for the Pd-V system.

It has also been shown that the GPM is equivalent to the embedded cluster method (ECM), originally proposed by Gonis [29]. The basic idea of the ECM is contained in Eq. (12) adapted to the second method of averaging described in Sect. 3:

$$\varepsilon^*_\alpha = \rho^*_{N-\alpha}\ \mathrm{Tr}^{(N-\alpha)}\ E(\sigma_\alpha;\ \sigma^*_{N-\alpha}) \qquad (16)$$

in which the notation $N-\alpha$ indicates that the normalization and the trace operation refer to configurations which exclude those of the cluster α. The energy ε^*_α, according to Eq. (21), is thus that of a cluster α, in a given configuration, embedded in a completely disordered medium of concentration c^*, since the trace pertains only to those configurations σ^* which have that particular concentration. In Gonis's ECM, the disordered medium is that of the single-site CPA. The ECM has been implemented on both TB [30] and KKR-CPA [31].

Very recently, Carlsson [32] has shown that the essentially concentration independent cluster interaction scheme of Connolly and Williams and the essentially concentration dependent pair interaction scheme of Gautier and Ducastelle can be related by expressing cluster concentrations by means of a superposition approximation. Nevertheless, the connection between the two methods has yet to be explored extensively.

5. CALCULATION OF PHASE DIAGRAMS

Thus far, only the zero temperature aspects have been considered. Our purpose, however, is to determine phase equilibria at arbitrary temperature. It is therefore required to include entropy contributions, both configurational and vibrational. At the moment, the latter is best taken into account by empirical means. The configurational entropy can be calculated quite accurately by the cluster variation method (CVM) [13]. The basic idea is to express the entropy functional

$$S[\rho] = - k_B \, Tr^{(N)} \, \rho \ln \rho \qquad (17)$$

in an approximate manner by means of partial densities defined in Eq. (6) [15]. These "cluster concentrations" themselves are linear combinations of the correlation functions ξ. Hence, in this approximation, the free energy functional turns out to be analytic in the independent variables ξ. The equilibrium free energy is then obtained by minimizing with respect to the cluster correlations ξ. In this way, free energy curves can be calculated for various phases of interest as a function of concentration c, at any desired temperature. Common tangents can then be constructed and phase equilibria determined.

It is seen, by Eqs. (8) and (13)-(15), that the energy E consists of a temperature independent part (E_{dis}) and a part (E_{ord}) which depends on temperature implicitly through the correlations ξ. Thus, the calculation of energy parameters ε_0 and ε_α, performed at O K, can be decoupled from the temperature dependent CVM calculations, thereby resulting in considerable simplification.

As an illustration of the method of calculating EPI's by perturbing the disordered state, we recently performed TB-CPA computations for the Ti-Rh system [33]. We assumed fixed fcc and bcc lattices with atoms occupying the lattice sites with no displacements allowed. The following Slater-Koster parameters were used: $dd\pi = \frac{3}{4}|dd\sigma|$, $dd\sigma = -1.385$, $dd\delta = 0$.

For the fcc electronic density of states (DOS), these values give a d-band width of 11.08 in canonical units (c.u.), with 1c.u.≈4.5eV for a typical d-band width of 5eV. The only element-specific parameters to enter the calculations are thus the number of d-electrons for element A (N_A) and for the element B (N_B), and the diagonal disorder δ_d proportional to the magnitude of the d-band energy difference between A and B. No non-diagonal disorder is considered. Charge transfer is not taken into account. Since differences of energy between ordered and disordered states are required, only band structure energy terms will be considered, under the assumption that double counting and electrostatic terms will cancel approximately. The resulting one-electron TB canonical band model with s and p electron contributions neglected is not expected to yield correct structural predictions for all pure elements across the transition metal series, but will prove to be serviceable for determining approximately the binary phase equilibria considered.

The statistical thermodynamical model employed was the CVM in the tetrahedron approximation: nn regular tetrahedron for fcc (α), irregular tetrahedron for bcc (β), comprising nn and nnn lattice vectors. The energy

E_{dis} [see Eq. (14)] was calculated by the single-site CPA, the Green's functions being calculated by the recursion method [34,35]. The GPM was then used to evaluate pair interactions $V_1^{\alpha}(nn)$ in the fcc case and $V_1^{\beta}(nn)$ and $V_2^{\beta}(nnn)$ in the bcc case as a function of concentration. Full accounts of the computational methods have been given elsewhere [36].

Minimization of the CVM free energy was performed for the disordered phases and also for various expected ordered superstructures of the parent lattices. Ordered superstructures of fcc are designated as α', α'', ..., superstructures of bcc are designated as β', β'' .... For the scheme of pair interactions used here, the ground states of order (superstructures) are fully known [1,2]: the $L1_2$ (Cu_3Au prototype) and $L1_0$ (CuAu I prototype) structures are expected for fcc, and the B2 (CsCl), B32 (NaTl), and DO_3 (Fe_3Al) structures are expected for bcc.

The number of d electrons valid for Ti is N_A=3 and for Rh, N_B=8. The diagonal disorder was somewhat arbitrarily set at δ_d=0.8. These were the only parameters required in the calculation of the fcc and bcc disordered state energies and pair interaction parameters as a function of concentration. Free energies for disordered phases and fcc and bcc based superstructures were then determined by the CVM.

When free energies of both fcc and bcc disordered and ordered phases were combined, the diagram of Fig. 1 was obtained. It is apparent that phase equilibria are dominated on the A (Ti) side by the bcc lattice, on the B (Rh) side, by the fcc lattice. The fcc + bcc ($\alpha+\beta$) two-phase region located at about 60% B must necessarily persist to infinite temperatures. In the center of the phase diagram, the B2 phase (bcc superstructure) overwhelms the $L1_0$ (fcc superstructure) for geometrical reasons: for dominant nn pair interaction, ordering is optimized in the bcc lattice (B2 ordered structure) whereas it is frustrated in the fcc lattice, the characteristic feature of that

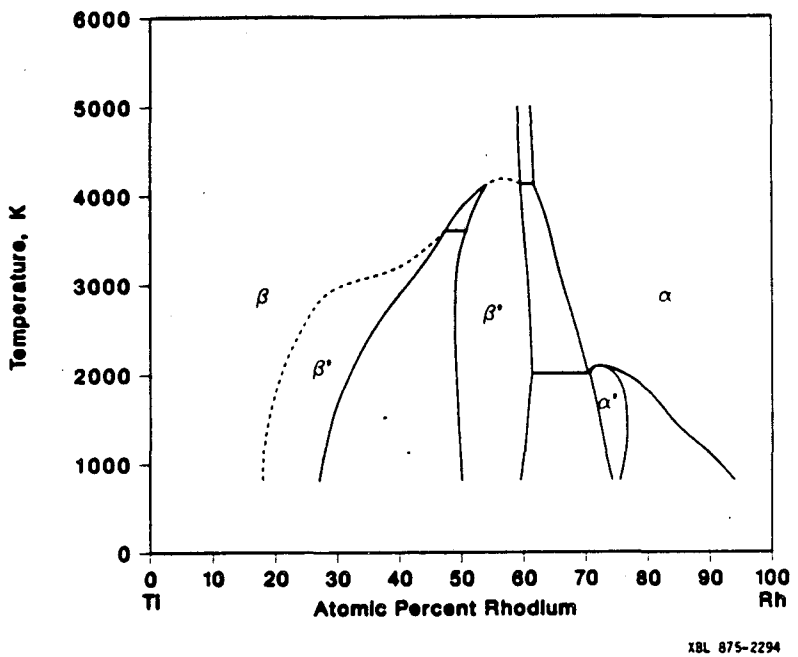

Fig. 1

lattice being the equilateral nn triangle for which only AAB or ABB partial order can be achieved. The ordered B2 (β') phase is found in two regions of the diagram: somewhat off-center (50 to 60% B) and way off stoichiometry. That latter feature may well be an artifact of the type of approximation used here for calculating nn and nnn bcc pair interactions. Second-order transitions (dashed lines), allowed by the Landau rules, are predicted at the top of the central B2 region and between the disordered β and the strongly off-stoichiometric β'. The α' superstructure ($L1_2$) located about the A_3B is separated from the parent disordered fcc (α) by first-order transitions, as expected. The locus of equality between the B2 and metastable $L1_0$ phases has also been plotted as a dot-dash curve in Fig. 1. It was found that, with diagonal disorder δ_d=0.6, the $L1_0$ phase becomes stable at low temperature and can coexist with B2. The temperature scale was fixed by adopting the canonical d-band width of 5eV.

Available experimental data on the Ti-Rh and Ti-Ir systems have been examined recently by Murray [37] and the resulting "assessed" phase diagram for Ti-Rh is shown in Fig. 2. Empirically determined phase diagrams for Ti-Ir, Zr-Rh and Zr-Ir are quite similar in their essential features, within the limits of experimental uncertainty. At first glance, theoretically (Fig. 1) and experimentally determined (Fig. 2) phase diagrams seem to differ markedly. It must be recognized however, that the scope of the present computation is a limited one: Only the two basic lattices, fcc and bcc were considered along

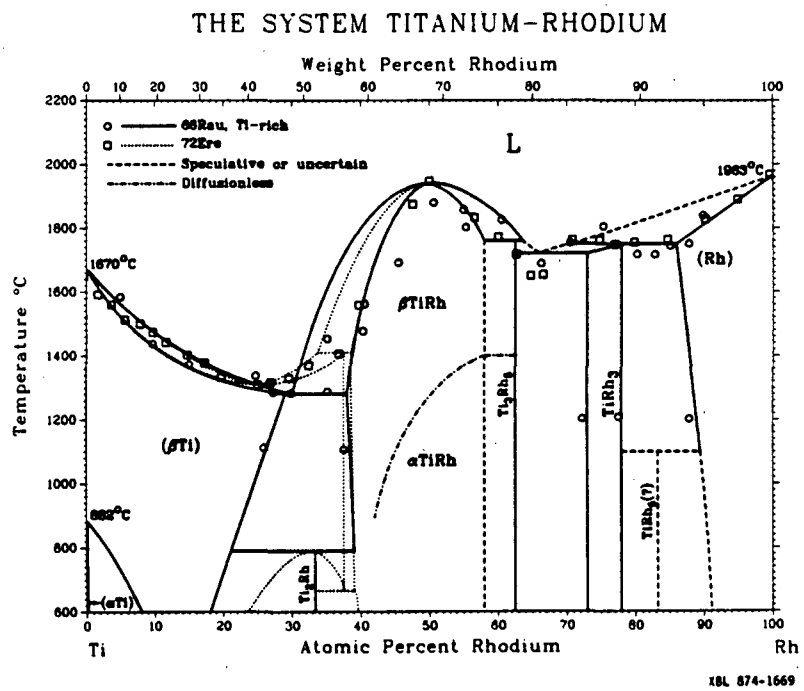

Fig. 2

with their allowed superstructures, i.e. a total of 11 possible phases was entered in the calculation. Out of these, the minimization procedure correctly predicts, at approximately correct location: the βTi phase, the βTiRh (β' in Fig. 1, correct B2 structure), and the $TiRh_3$ (α' in Fig. 1, correct $L1_2$

structure). The region marked "αTiRh" on the experimentally-determined phase diagram (Fig. 2) is separated from βTiRh by a dot-dash curve which pertains to a "diffusionless transformation". Thus, αTiRh is a metastable phase, of uncertain crystal structure, but described generally as "distorted $L1_0$". As mentioned above, in the calculation, $L1_0$ is marginally unstable, but becomes stable for δ_d=0.6. Our own predicted line of marginal stability for $L1_0$ is the (α''/β') dashed curve of Fig. 1, not too far off the experimental one, considering the uncertainties in both calculated and experimental determinations.

Experimentally observed, but imperfectly characterized "interloper" phases Ti_2Rh (Laves phase), Ti_3Rh_5, and $TiRh_5$ could not be predicted by the present model since these phases have crystal structures not contained in the set of possible superstructures of fcc or bcc, and were therefore not included in the calculation. Likewise, αTi (hcp) was not "coded in", but is certainly not a prominent feature of the phase diagram. Actually, agreement with the Ti-Ir experimental diagram is better, since the missing A_2B, A_3B_5 and AB_5 are not observed in that system. There exists, however, a stoichiometric A15-type phase Ti_3Ir.

The only phase incorrectly predicted by the model is the far off-stoichiometric β' (B2). However, note that the transition from β to β' is calculated to be second order so that, at such low concentrations, β' may have been missed altogether in experimental investigations. Furthermore, there exists considerable discrepancy in the experimental findings: the (βTi)/(βTiRh) two-phase boundaries differed so much from one experimental investigation to another that Murray [37] was compelled to superimpose the two conflicting versions in the assessed diagram. The two experimental determinations differ from one another by at least as much as one of these does from the theoretical prediction.

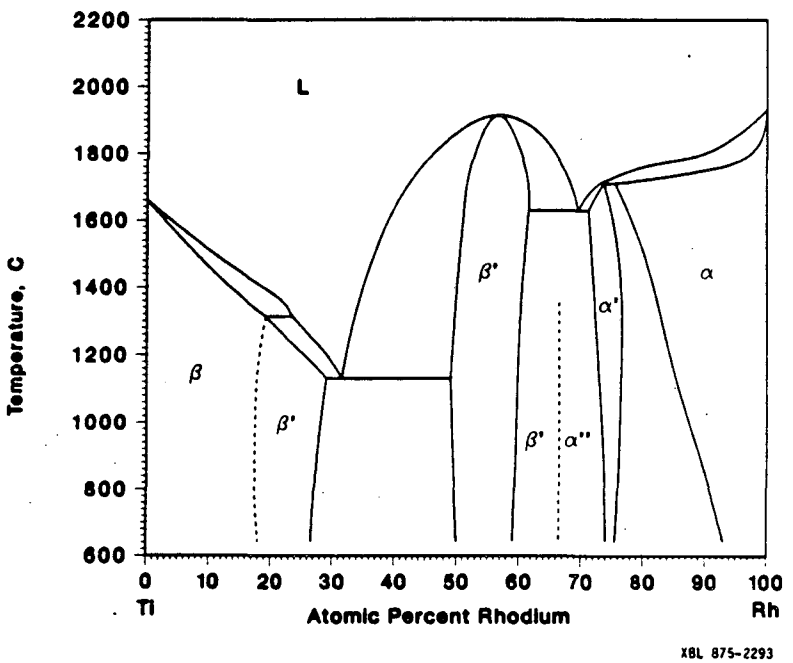

Fig. 3

The most flagrant shortcoming of the calculated diagram is, of course, the absence of liquid-phase equilibria. Such a deficiency cannot be remedied at present due to the absence of reliable and tractable models of liquid alloys. Consequently, and simply for the sake of illustration, we constructed an empirical liquid free energy function, based on a sub-regular solution model the parameters of which were fitted to provide the correct pure Ti and pure Rh melting temperatures and the βTiRh congruent melting temperature. Experimentally determined [38] values of Ti and Rh entropies of melting were included. The fitted liquid free energy was then combined with calculated (parameter-free) crystalline phase free energies to produce the phase diagram of Fig. 3. The agreement between theory and experiment is now much more striking. We repeat, only the liquidus-solidus curves resulted from parital fitting; all other phase equilibria lives were calculated from the TB-CVM model with no adjustable parameters.

6. Conclusion

Electronic band structure calculations are becoming increasingly accurate and reliable. It is thus timely to make use of the modern first principles techniques to calculate alloy properties by combining quantum mechanical with statistical mechanical calculations. Various schemes for performing such combined computations have been described briefly here. One example was given, that of the calculation of the Ti-Rh phase diagram by means of a fairly crude TB-CPA method.

The results of that and other calculations suggest that prediction of thermodynamic properties by *ab initio* procedures will soon become a reality. Many problems remain to be solved, however, such as that of elastic energy contributions, vibrational entropy, extension of the methods to more complex intermetallic phases and to the liquid state, generalization to multicomponent systems, etc... If the calculations can be made truly element-specific and if some of the difficulties already encountered can be overcome, we should soon have computational techniques capable of producing thermodynamic values for alloy systems of interest. If that comes to pass, Materials Science will have acquired real predictive value.

Acknowledgements

Calculations of the Ti-Rh system were performed by Drs. M. Sluiter and P. Turchi, supported by a grant from the Lawrence Livermore National Laboratory. The author wishes to thank Dr. J. L. Murray for having supplied him with a copy of Ref. 37 prior to publication. The research was supported, in part, by the Director Office of Energy Research, Materials Sciences Division, U.S. Department of Energy, under Contract No. DE-AC03-76SF00098.

REFERENCES

1. Kanamori, J., Prog. Th. Phys., 1966, 35, 16.

2. Allen, S. M. and Cahn, J. W., Acta Metall., 1972, 20, 423; Scripta Metall., 1973, 7, 1261.

3. Kanamori, J., Solid State Comm., 1984, 50, 363.

4. Kanamori, J. and Kakehashi, Y., J. Phys., 1977, 38, C7-274.

5. Finel, A., Thèse de Doctorat d'Etat, Univ. Pierre et Marie Curie, Paris, 1987.

6. Kudo, T. and Katsura, S., Prog. Th. Phys., 1976, 56, 435.

7. Sanchez, J. M. and de Fontaine, D., in "Structure and Bonding in Crystals," Vol. II, pp. 73-274, Acad. Press, NY, 1981.

8. de Fontaine, D., in "Solid State Physics," Vol 34, Acad. Press, NY, 1981.

9. Sanchez, J. M., Gratias, D. and de Fontaine, D., Acta Cryst., 1982, A38, 214.

10. Khachaturyan, A. G., "Theory of Structural Transformations in Solids," Wiley-Interscience, NY, 1983.

11. Pettifor, D. G., New Scientist, May 29, 1986, p. 48.

12. Binder, K., Lecture Notes, NATO Adv. Study Inst. on Alloy Phase Stability, Crete 1987 (in press).

13. Kikuchi, R., Phys. Rev., 1951, 81, 988.

14. van Baal, C. M., Physica, Utrecht, 1973, 64, 571.

15. Sanchez, J. M., Ducastelle, F. and Gratias, D., Physica (Amsterdam), 1984, 128A, 334.

16. Sanchez, J. M. and de Fontaine, D., Phys. Rev. B, 1980, 21, 216.

17. de Fontaine, D., in "High-Temperature Ordered Intermetallic Alloys," pp. 43-64, MRS Symposia Proceeding, Vol. 39, 1985.

18. Sigli, C. and Sanchez, J. M., Calphad, 1984, 8, 221.

19. Gautier, F., Ducastelle, F. and Giner, J., Phil Mag., 1975, 31, 1373.

20. Velicky, B., Kirkpatrick, S. and Ehrenreich, H., Phys. Rev., 1968, 175, 747.

21. Stocks, G. M., Williams, R. W. and Faulkner, J. S., Phys. Rev. B, 1971, 3, 4390.

22. Johnson, D. D., Nicholson, D. M., Pinsky, F. J., Gyorff, B. L. and Stocks, G. M., Phys. Rev. Lett., 1986, 56, 2088.

23. Connolly, J. W. D. and Williams, A. R., Phys. Rev. B, 1983, 27, 5169.

24. Terakura, K., Oguchi, T., Mohri, T. and Watanabe, K., Phys. Rev., 1987, 35, 2169.

25. Mbaye, A. A., Ferreira, L. G. and Zunger, A., Phys. Rev. Lett., 1987, 58, 49.

26. Bieber, A. and Gautier, F., Acta Metall., 1986, 34, 2291.

27. Sigli, C., Kosugi, M. and Sanchez, J. M., Phys. Rev. Lett., 1986, 57, 253.

28. Turchi, P., Gonis, A. and Stocks, G. M., Phys. Rev. Lett., to be published.

29. Gonis, A. and Garland, J. W., Phys. Rev. B, 1978, 18, 3999.

30. Gonis, A. and Garland, J. W., Phys. Rev. B, 1977, 16, 2424.

31. Gonis, A., Stocks, G. M., Butler, W. H. and Winter, H., Phys. Rev. B, 1984, 29, 555.

32. Carlsson, A. E., Phys. Rev. B, 1987, 35, 4858.

33. de Fontaine, D., Sluiter, M. and Turchi, P., in "Phase Transformations," 1987, Inst. of Metals, London (in press).

34. Turchi, P., These de Doctorat d'Etat, University Paris VI, 1984.

35. Haydock, R., Sol. St. Physics, Eds., H. Ehrenreich et al., Academic Press, 1980, Vol. 35, 214.

36. Turchi, P., Sluiter, M. and de Fontaine, D., Phys. Rev. B, 1987, 36, 3161.

37. Murray, J. L., Bull. Alloy Phase Diag., 1982, 3, 335; and to be published in "Titanium Binary Phase Diagrams," ASM.

38. Hultgren, R. "Thermodynamic Properties of Alloys," 1963, J. Wiley and Sons, NY.

FIGURE CAPTIONS

1. Calculated phase diagram for Ti-Rh-like binary systems. The miscibility gap between fcc and bcc disordered phases persists to infinite temperatures (in the absence of melting).

2. Assessed Ti-Rh phase diagram according to Ref. 40.

3. Phase diagram calculated as in Fig. 1 but with fitted free energy curve for the liquid phase included. Phases are: L=liquid, α-fcc (disordered), α'=$L1_2$, β=bcc (disordered), β'=B2, α''=$L1_0$ (metastable).

LAWRENCE BERKELEY LABORATORY
TECHNICAL INFORMATION DEPARTMENT
UNIVERSITY OF CALIFORNIA
BERKELEY, CALIFORNIA 94720